Prediction of Optical Density using CFD

HAUKUR INGASON AND BROR PERSSON,
Swedish National Testing and Research Institute (SP)
Box 857, S-501 15 BORÅS, Sweden

ABSTRACT

In the present work theoretical models for determining optical density in smoke (visibility) with Computational Fluid Dynamics (CFD) simulations are compared to experimental data. CFD models do not give the smoke concentration directly in the calculation domain. Two different methods are used in the paper to convert the CFD results into an optical density. The first model analysed here assumes that the optical density is dependent on the local conditions in the flow field and the mass optical density of the burning material. Good correlation was found between calculated results based on the model and the experimentally obtained results. A second model is based on the assumption that there is a correlation between the gas temperature rise and the optical density. This model produced poorer results, especially far away from the fire source. The experimental test rig consisted of a 20 m long tunnel (corridor/culvert) with different types of longitudinal ventilation and exhaust ventilation arrangements. The optical density was measured at three different distances downstream of a kerosine fire source.

KEYWORDS: CFD, optical density, visibility, optical mass density, smoke concentration, kerosine pool fire

INTRODUCTION

The generation of smoke in fires is generally associated with reduction in visibility and exposure to toxic environments. In fires, reduction in visibility due to smoke often leads to a critical situation for escaping people. Due to toxic gases and high temperatures the situation may be very hazardous if people are not quickly able to find their way to a safe place. Since CFD models are commonly used in the design of escape routes, especially in underground constructions like tunnels and underground stations, a reliable smoke model is essential for their design. CFD models calculate numerically the conservation of mass, momentum and

energy in an arbitrary number of control volumes. The number of control volumes typically ranges from thousands up to several hundred thousands. The output from the CFD models usually consists of temperatures, velocities and mass fractions of oxygen (O_2), carbon dioxide (CO_2) and fuel. Optionally a conserved scalar can be applied. Hence there is no direct correlation between optical density in smoke (or visibility) and the values obtained by the CFD models. Therefore, there is a need for a transformation model that uses the output from the CFD model and recalculates it into some useful figure that can be converted to visibility in smoke.

Validated engineering models for determining optical density in connection with CFD simulations are lacking. Estimates by coupling the mass fraction of the combustion products (CO_2) [1, 2] or decreases in the oxygen mass fraction (O_2) [3, 4] have been used. Another approach is to treat the soot (smoke) as an inert gas described by a conserved scalar by assuming that a certain fraction of the fuel is converted to soot [10]. There is still a lack of validation of these models for use in CFD calculation.

Recently, Ingason and Persson [5] presented a simple theoretical model aimed to tackle this problem with a more rigorous approach. The work was aimed at extending the models reported in [1, 4]. The results were found to be very encouraging. The experimental conditions were rather rough so there is still a need for testing under more well defined conditions. In the Ingason and Persson [5] study the experimental site consisted of a 100 m long blasted rock tunnel with a cross sectional area of 2.7 m by 3 m. The fire load used (1 - 1.5 MW) was located 60 m from a 13 m high chimney located at one end of the tunnel. The other end of the tunnel was fully open. Two different fuels were used; heptane and wood cribs. The mass optical density for each fuel and configuration had been determined using a laboratory hood system, in which the fuel and fuel configuration were identical to that in the tunnel experiments. The optical density was measured at three different heights (1 m, 2 m and 2.65 m above floor) 49 m downstream of the fire using specially engineered smoke density meters [6]. The smoke density was measured as the optical density of smoke over the path of 1 meter. At the same locations the oxygen and gas temperature were measured. Instead of using CFD results the measured oxygen concentration and gas temperature were used as input to calculate the optical density. The calculated values were then compared to the measured optical density using the smoke density meter. The results were found to be very encouraging for the two fuel types used. There was a slight difference between measured and calculated peak values for the wood crib test.

There is still a need for more validation tests for the model presented in [5]. In the present study a comparison between the model and new test data is presented. Further, comparison with a model similar to that found in [7] for detectors is also compared with the experimental data. The model in [7] assumes that there is a well-defined correlation between the temperature rise and the smoke concentration. This is probably acceptable where heat losses are negligible.

MODELS FOR ESTIMATION OF OPTICAL DENSITY FROM CFD CALCULATIONS

In the following, equations used for comparison of measured and calculated results are derived. The theoretical approach given here is based on the work presented in References [5] and [8].

Visibility is reduced because only a certain fraction of light can pass through the smoke due to light absorption and scattering and because of the irritant compounds present as fire products. The optical density D is defined as [8]

$$D = \log(I_0 / I) \tag{1}$$

where I_0 is the initial intensity of light (arbitrary units) and I is the final light intensity after passing through a smoke layer of thickness l. The fraction of the light passing through the smoke layer is expressed as

$$I / I_o = e^{(-\sigma \cdot l)} \tag{2}$$

Here σ is the extinction coefficient (m^{-1}), which is a function of the mass concentration of smoke, C_s. The optical density per unit optical path length can then be expressed

$$D / l = \xi \cdot C_s \tag{3}$$

where C_s is in kg/m^3 and ξ is the specific extinction coefficient of smoke or particle optical density (m^2/kg). For an open system, the smoke mass concentration takes the form

$$C_s = Y_s \dot{G}_f / \dot{V}_T \tag{4}$$

where Y_s is the yield of smoke (g/g), $\dot{G}_f$ (g/s) denotes the mass flow of material vapours of the burning material and $\dot{V}_T$ is the total local volumetric flow rate of the mixture of fire products and air (m^3/s). Combining eqs. (3) and (4) gives

$$D / l = \xi \cdot Y \cdot \dot{G}_f / \dot{V} \tag{5}$$

The parameter ξY_s is defined as mass optical density, D_{mass} (m^2/g) and is compiled in [8] for a number of different materials.

Optical Density based on mass fraction of oxygen

To apply equation (5) to CFD results it is necessary to express the ratio $\dot{G}_f / \dot{V}_T$ in terms of local variables appearing in the CFD simulation. On that account it is assumed that the ratio can be approximated as [5]

$$\dot{G}_f / \dot{V}_T = \Delta G_f / \Delta V \tag{6}$$

i.e. the ratio is approximated by the local density of material vapours. The amount of fuel involved in the generation of smoke within the control volume is assumed to be directly proportional to the amount of oxygen consumed. In the first approximation the amount of unburned fuel is neglected. Let Y_o denote the local mass fraction of oxygen (oxidant), $Y_{o\infty}$ the mass fraction in undisturbed air and r_o the stoichiometric oxygen to fuel ratio. The amount of fuel can then be expressed

$$\Delta G_f = \rho(Y_{O\infty} - Y_O)\Delta V / (Y_{O\infty} + r_O) \tag{7}$$

Thus, the optical density per path length of smoke can be written

$$D / l = D_{maxs} \cdot \rho \cdot (Y_{o\infty} - Y_o) / (Y_{o\infty} + r_o) \tag{8}$$

Here the local density $\rho = \rho_0 T_0 / T_g$ and the local mass fraction of oxygen Y_o can be obtained from CFD results. T_g is the local gas temperature and $\rho_0 T_0$ are corresponding ambient conditions. The stoichiometric oxygen to fuel ratio, r_o, can be obtained theoretically or experimentally for each fuel. The mass optical density, D_{mass}, can be taken from reference [8] or from experiments like the one given in [5], see Table 2.

Optical Density Based on Mass Fraction of Combustion Productions

Equation (8) can alternatively be formulated in terms of the local mass fraction of combustion products rather than the mass fraction of oxygen. Thus,

$$\Delta G_f = \Delta G_p / (1 + r_0) = \rho \Delta V Y_p / (1 + r_0) \tag{9}$$

where index p indicates combustion products. If we assume that the combustion products consist of CO_2 we can rearrange equation (9) with aid of equations (5) and (6)

$$D / l = D_{maxs} \cdot \rho \cdot Y_{co2} / (1 + r_o) \tag{10}$$

Optical Density Based on Temperature

If heat losses to surrounding walls are negligible ΔG_f can be formulated in terms of local temperature differences,

$$\Delta G_f = \rho \Delta V C_p \Delta T_g / (\alpha H_c) \tag{11}$$

using the energy equation ($Q_c = \rho \dot{V}_T C_p \Delta T_g$) and the relationship $Q = G_f H_c$. Here C_p is the heat capacity, Q_c, convective heat release rate, Q chemical heat release rate, H_c the heat of combustion and α the ratio Q_c/Q. Thus using equation (5) and (6) and $\rho = \rho_0 T_0 / T_g$ we obtain

$$D / l = D_{mass}\left(C_p \rho_0 T_0 / \alpha H_c\right)\Delta T_g / T_g \qquad (12)$$

EXPERIMENTAL SET-UP

In order to validate equations (8), (10) and (12) smoke spread tests were performed in a model tunnel (corridor, culvert) measuring 2 m wide, 1 m high and 20 m long. The material of the walls, floor and ceiling consisted of a 12 mm Promatec fibre-silica board - except for one side-wall which consisted of 5 mm thick fire resistance window glass. The window was used to visually observe the smoke spread. The fire load consisted of a Kerosine pool fire located 2.5 m from one end of the tunnel (location D in Figure 1). Two different pan sizes were used, 0.33 x 0.33 m and 0.4 x 0.4 m, respectively. The ventilation arrangement and the longitudinal ventilation were varied. Different types of shafts (various height and width) were mounted along the tunnel (in locations A, B or C, see Figure 1). The main objective of test series was to investigate the influence of longitudinal ventilation on the efficiency of the thermal ventilation in tunnels/culverts through shafts. In this study the optical density versus the temperature and oxygen mass fraction is analysed separately.

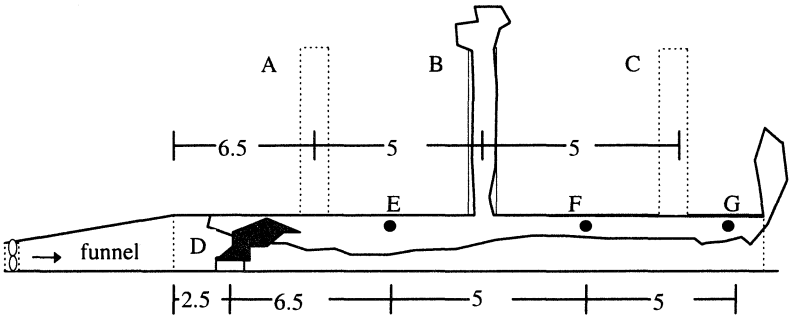

FIGURE 1. The experimental set-up. All dimensions are in metres. The fire source is located at D.

A specially designed funnel shaped tunnel was attached to one end of the tunnel in order to create a uniform flow over the cross-section at the tunnel entrance, see Figure 1. The other end of the tunnel was fully open. Extensive work was put on creating a uniform air flow over the tunnel cross-section. Measurements of the optical density, temperatures and oxygen concentrations were performed at three different locations downstream of the fire, locations E, F and G, see Figure 1. The measuring points E, F and G were placed 0.25 m below the ceiling. The optical density was measured with optical density meters (photocell and lens) over the path length of 2 m. The oxygen concentration was measured at a point 0.25 m below the ceiling and along the centreline of the tunnel. The temperature used in the calculations is an average measurement of two centreline temperatures at 0.2 and 0.3 m below ceiling,

respectively. The thermocouples were of type K with a wire diameter of 0.25 mm, chromel-alumel, 1200 °C range. Oxygen concentrations were measured by sucking the gases through a probe consisting of copper tube (Ø 6 mm) to an analyser.

The optical density is measured over the entire width of the tunnel whereas the oxygen and temperature are measured at a point. This may introduce an error in the validation when the measured values using the optical density meter are in fact an average value while the calculated values using oxygen and temperature are based on point measurements. Preliminary measurements indicate, however, that the temperature and oxygen concentration are quite uniform over the width of the tunnel. The variation is mainly in the vertical direction.

In order to measure the mass burning rate the Kerosine fuel pan was placed on a weighing platform located under the Promatec floor. Extensive work was carried out to obtain a steady mass burning rate during the pool fire tests. Usually the rim of a fuel pan will warm up and the heat balance at the fuel surface will be continuously changing. This will lead to a mass burning rate curve which is unsteady during the fire test. For small fuel pans this can be a great problem. The simplest way to obtain steady state conditions is by controlling the heat balance at the fuel surface. This can be done by cooling the rim by circulating water. The problem is to find the appropriate geometry of the rim and an appropriate rate of water flow.

After extensive work it was found that for the square pans used the best results were obtained with a water flow rate of 2 litre/minute and a cross sectional area of the rim of 15 mm wide by 50 mm high. The rim it self consisted of a U-profile measuring 15 mm x 40 mm with a 330 mm x 330 mm (or 400 mm x 400 mm) steel sheet (the bottom of the fuel pan) welded to the U-profiles. In order to avoid fuel leaking over the edge of the rim a 10 mm high steel edge was welded on the top of the rim. Thus, the height of the inner surface of the pan was 50 mm. The water cooled part was 40 mm. The thickness of the steel used in the rim was 2 mm. The temperature of the water flowing into the rim of the fuel pan was 10 °C and the water temperature flowing out from the rim was about 30 - 35 °C. In Figure 2, typical mass burning rate curves are shown for two different pan sizes. This method is found to be very robust and cheap. The mass burning rate become steady after only 1-2 minutes.

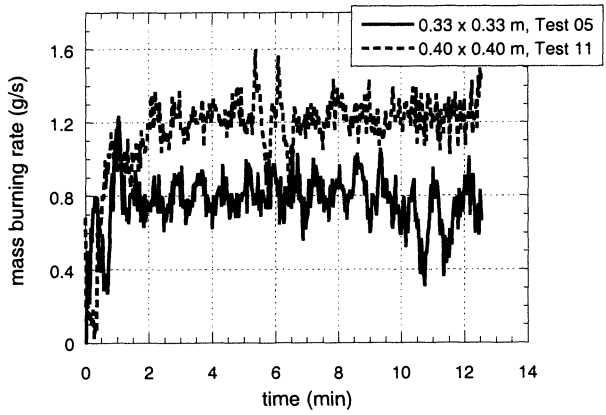

FIGURE 2. Mass loss rate measured with water cooled rims. Result using two different pan sizes are shown, 0.33 m x 0.33 m and 0.40 m x 0.40 m, respectively.

The longitudinal ventilation (air velocity) inside the tunnel was varied. In order to establish a uniform flow a fan was attached to the tunnel, see Figure 1. Four different air velocities were used in the test series, 0, 0.5, 0.75 and 1 m/s. Different arrangements of shafts were used in the test series, see Table 1. The number and size of the shafts were also varied. The heat release rate was determined by multiplying the average mass burning rate with the heat of combustion of H_c=39.5 kJ/g for Kerosine. This value was obtained by direct measurement in a Cone Calorimeter [9].

TABLE 1. The experimental program.

Test nr	Air velocity (m/s)	Shaft (height/width)	Number of shafts	Fire source (m x m)	Average $\dot{m}_f$ (g/s)	$\dot{Q}$ (kW)
01	0	1/0.4	3	0.33 x 0.33	0.97	38.3
02	1	--- " ---	--- " ---	--- " ---	1.07	42.3
03	0	3/0.4	--- " ---	--- " ---	0.83	32.7
04	0.5	--- " ---	--- " ---	--- " ---	0.78	30.9
05	0.75	--- " ---	--- " ---	--- " ---	0.76	29.9
06	1	--- " ---	--- " ---	--- " ---	1.04	40.9
07	0	--- " ---	--- " ---	0.4 x 0.4	1.35	53.4
08	1	--- " ---	--- " ---	--- " ---	1.39	54.9
09	0.75	--- " ---	--- " ---	--- " ---	1.27	50.3
10	0.5	--- " ---	--- " ---	--- " ---	1.18	46.6
11	0.5	3/0.4 (location B)	1	--- " ---	1.23	48.7
12	0.75	--- " ---	--- " ---	--- " ---	1.24	49.0
13	1	--- " ---	--- " ---	--- " ---	1.49	59.0
14	0	--- " ---	--- " ---	--- " ---	1.82	71.9
15	0.5	3/0.2	--- " ---	--- " ---	1.22	48.3
16	1	--- " ---	--- " ---	--- " ---	1.77	70.0
17	0	closed	0	--- " ---	2.01	79.4
18	1	--- " ---	--- " ---	--- " ---	1.45	57.4
19	0.75	--- " ---	--- " ---	--- " ---	1.25	49.2
20	0.5	--- " ---	--- " ---	--- " ---	1.31	51.8
21	0	--- " ---	--- " ---	0.33 x 0.33	0.86	33.9
22	1	--- " ---	--- " ---	--- " ---	1.04	41.0
23	0.75	--- " ---	--- " ---	--- " ---	0.76	29.9
24	0.5	--- " ---	--- " ---	--- " ---	0.77	30.3
25	0.5	3/0.6	1	0.4 x 0.4	1.30	51.3
26	1	--- " ---	--- " ---	--- " ---	1.41	55.9

4 RESULTS

The parameters, D_{mass} and r_0, for the Kerosine were first determined from measurements in a hood system. The hood system consisted of an exhaust duct and a hood located above the fire [9]. The hood size was 3 m x 3 m with the lowest point 2.5 m from the floor. Total chemical heat release rate and the mass burning rate of the fuel were measured. In the exhaust duct the volume flow, $\dot{V}_T$, gas temperature, T_g, gas concentrations, O_2, CO_2, CO and intensity of light, I, were measured. These data were used to determine the mass optical density, D_{mass}, and the stoichiometric oxygen to fuel ratio, r_o, for Kerosine. D_{mass} was determined by combining equations (1) and (5) or

$$D_{mass} = (\log(I_0 / I) / l) \cdot (\dot{V}_T / \dot{G}_f) \tag{13}$$

where $\log (I_0/I)$ and $\dot{V}_T$ are determined from measurements in the exhaust duct. $\dot{G}_f$ is determined by measuring the mass loss rate of the fuel. The path length of smoke in the exhaust duct was l=0.4 m. Since the oxygen mass fraction, Y_0, and the gas temperature, T_g, is

measured in the exhaust duct and D_{mass} is independently determined from equation (13) we can use equation (8) to determine r_0 for Kerosine. The obtained values were D_{mass}=315 m^2/kg and r_0=3.08.

The next step is to compare the measured optical density per unit path length of smoke, D/l, in the tunnel with the calculated values obtained from equation (8). The optical density is determined with aid of equation (1) using measured values of I and I_0 and a path length, l = 2.0 m. The "calculated" values of D/l were obtained by using the measured oxygen mass fraction, Y_{o} and the gas temperature, T_g, in the tunnel as well as the D_{mass} and r_o obtained from the hood tests. Thus, if the model is appropriate we should obtain similar results between measured and "calculated" values at the measurement stations E, F and G for all the tests conducted. The model does not take into account any smoke coagulation or deposition of smoke on walls. In figure 3 the results of the measured and the "calculated" values are presented for locations E, F and G. The agreement is very good. Thus, if CFD can calculate the local density of the fuel and gas concentrations (O_2 or CO_2) the optical density could be calculated with reasonable accuracy provided that reliable information is available about the mass optical density, D_{mass}.

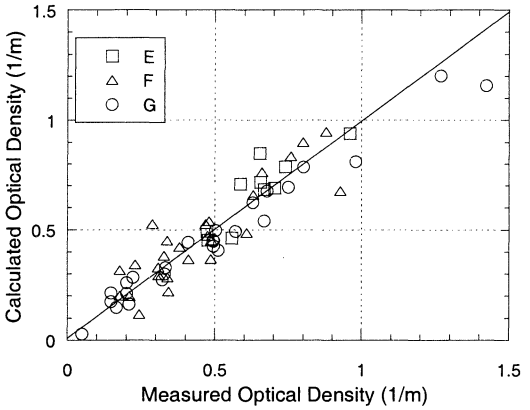

FIGURE 3. Calculated optical density using equation (8) versus measured optical density per unit path length of smoke using an optical density meter at three different locations E, F and G.

The CO_2 was not measured in the test series but there should not be any difference in the results based on equation (10) or (8) as long as the fire is well-ventilated. The amount of CO_2 produced is usually directly proportional to the amount of oxygen consumed.

Comparison of the optical density obtained by equation (12) and measured Optical Density with an optical density meter was also carried out. The ratio α was measured for Kerosine in the hood test; 0.6, C_p is assumed to be 1 kJ/kg K and H_c=39.5 MJ/kg (measured in the hood tests and in the Cone Calorimeter). The results are shown in Figure 4.

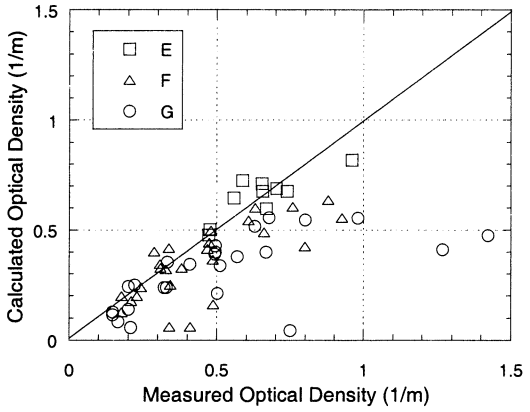

FIGURE 4. Calculated optical density using equation (12) versus measured optical density using an optical density meter at three different locations E, F and G.

The model is based on the assumption that there is a well-defined correlation between the temperature rise and the optical density. This assumption is, as the results show, conceptually wrong. The system loses considerable amount of internal energy to the surrounding walls. If the calculations are based on the total amount of oxygen consumed or on assuming that a certain amount of the fuel is converted to smoke the system can be described by a conserved scalar. This explains why equation (12) produced poorer results than equation (8) and (10), especially far away from the fire source where the accumulated heat losses are considerable.

VISIBILITY

The practical use of the models presented here is the calculation of visibility in order to determine distance between escape routes. Since the model appears to work satisfactorily for different types of fuels it is conjectured that it will work for real fire loads as well.

There is not much information available in the literature on mass optical density, D_{mass}, for real fire loads. Tewarsson [8] presents an extensive list for a variety of fuels. In Table 2 values of D_{mass} for different types of vehicles are given based on large scale tests [10]. As can be seen in Table 2 there is a considerable variation in smoke production depending on type of vehicle. By using appropriate results from CFD calculations and D_{mass} from Table 2 and assuming a value for r_0 ($\approx$ 3-3.5 for most simple hydrocarbon fuels) one could easily obtain a mapping of the visibility in a tunnel or car parking garage. In reference [8], a relationship between optical density, D/l, and visibility is given. A visibility of 10 m is often used as a critical limit. It

corresponds to a visibility below which the safe evacuation of people will be difficult [3]. This corresponds to an optical density of about 0.13 m^{-1}.

TABLE 2. Mass optical density from burning vehicles in experiments given in [10]. The values given here are recalculated from data presented by Steinert [10].

Type of vehicle		Mass optical density, D_{mass} (m^2/kg)
	car (steel)	381
Road	car (plastic)	330
	buss	203
	truck	76-102
	subway (steel)	407
	subway (aluminium)	331
Rail	IC-type (steel)	153
	ICE-type (steel)	127-229
	2 joined ½ vehicles (steel)	127-178

Now we have an engineering tool for determining the visibility in fires depending on the fuel load. The problem is still to determine r_0 but it does not vary greatly for fuels found in vehicle fires (assuming mostly hydrocarbon fuels).

CONCLUSIONS

Theoretical models for determining the optical density in smoke using Computational Fluid Dynamics (CFD) calculations are compared to experimental data. Good correlation was found between calculated results and the experimentally obtained results. The model is based on the assumption that the optical density is dependent on the local conditions in the flow field and the mass optical density of the burning material. This indicates that if the local density and gas concentrations could be correctly predicted with CFD then it would be possible to calculate the visibility at different locations in a building or underground construction for different types of fuels.

A model based on the assumption of correlation between the rise of the gas temperature and the optical density was also investigated. This model produced poorer results, especially far away from the fire source.

REFERENCES

1. Kumar, S., Field Model Simulations of Vehicle Fires in a Channel Tunnel Shuttle Wagon, Fire Safety Science, Proceedings of the Fourth International Symposium, pp. 995-1006, 1997.

2. Nam, S., and DeGiorgio, A., CFD Applications to smoke movement in clean room environments based on CO2 concentration, Proceedings Second International Conference on Fire Research and Engineering, 3-8 August 1997, Gaithersburg, Maryland, USA.

3. Andersson, P., and Holmstedt, G., CFD Modelling Applied to Fire Detection-Validation Studies and Influence of Background Heating, 10. Internationale konferenz uber Automatische Brandentdeckung, AUBE 95, Duisburg, Germany, pp 429-438.

4. Tuovinen, H., Sensitivity Calculations of Tunnel Fires, Fire Technology, Vol 32, No 2, 1996.

5. Ingason, H., and Persson, B., Prediction of Visibility in Tunnel Fires, Safety in Road and Rail Tunnels, Third International Conference, Nice, France, 9-11 March 1998.

6. Hägglund, B., Jansson, R., and Nireus, K., Smoke Filling Experiments in a 6x6x6 meter Enclosure, FOA Rapport, C 20585-D6, September 1985.

7. Evans, D.D., and Stroup, D.W., Methods to calculate the response time of heat and smoke detectors installed below large unobstructed ceilings, NBSIR 85-3167, US Dept. Of Commerce 1985.

8. Tewarson A., "Generation of heat and chemical compounds in fires", SFPE Handbook, Section 1/Chapter 13, 1988.

9. Babrauskas, V., and Grayson, S., Heat Release in Fires, Elsevier Applied Science, 1992.

10. Proceedings of the International Conference on Fires in Tunnels, Swedish National Testing and Research Institute, SP-Report 1994:54.